Formation of the Oxanickelacyclopentene Complex from Nickel(0), Carbon Dioxide, and Alkyne. An *ab initio* MO/SD-CI Study. Part II.[1] Reactivity and Regioselectivity of Hydroxyacetylene

Shigeyoshi Sakaki,* Kazuya Mine, Taisuke Hamada, and Toru Arai#

Department of Applied Chemistry, Faculty of Engineering, Kumamoto University, Kurokami, Kumamoto 860

(Received December 26, 1994)

The formation reaction of oxanickelacyclopentene from [Ni(PH_3)], hydroxyacetylene (a model of ethoxyacetylene), and carbon dioxide was investigated by the ab initio MO/SD-CI method. Of the two possible products of oxanickelacyclopentene [(H_3P)Ni–C(OH)=CH–CO(O)] and [(H_3P)Ni–CH=C(OH)–CO(O)], the former was yielded with a lower activation energy (E_a) of 27 kcal mol^{-1} and a higher exothermicity (E_{exo}) of 31 kcal mol^{-1} than the latter (E_a=38 kcal mol^{-1} and E_{exo}=25 kcal mol^{-1}). This result is consistent with the regioselectivity experimentally observed in the Ni(0)-catalyzed 2-pyrone synthesis from ethoxyacetylene and carbon dioxide. The regioselectivity of this reaction and the reactivity of hydroxyacetylene are discussed in terms of the energy level and the shape of the hydroxyacetylene π^* orbital.

In various CO_2 fixation reactions,[2] the transition metal-catalyzed coupling reactions of CO_2 with unsaturated hydrocarbons are of particular interest,[3—7] because these kinds of reactions afford useful organic products such as 2-pyrone derivatives[3—6,8] and acrylic acid derivatives.[7] When unsymmetrically substituted acetylene is used as a substrate, interesting regioselectivity is observed in these coupling reactions; for instance, α-substituted acrylic acid **1** is preferentially produced from a terminal alkyne and CO_2 in the Ni-catalyzed electrochemical reaction (Eq. 1); **1** : **2**=90 : 10 for R=n-C_6H_{13}.

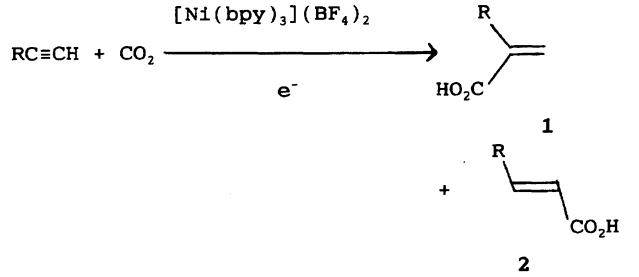

(1)

This reaction is believed to proceed via oxanickelacyclopentene **3** (Scheme 1), which has been isolated from the reaction between CO_2 and 4-octyne.[7d] In the case of a terminal alkyne, there are two isomers of **3**. The

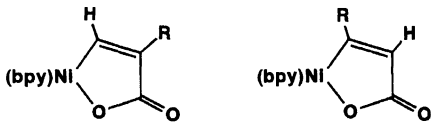

3a **3b**

Scheme 1.

preferential formation of **1** means that **3a** is more easily produced than **3b**. Another example is found in the Ni(0)-catalyzed coupling reaction of CO_2 with ethoxyacetylene, in which 2-pyrone derivative **7** is formed as a product (see Scheme 2). Of the two isomers of **7**, only 4,6-diethoxy-2-pyrone **7a** is produced; 3,5-diethoxy-2-pyrone **7b** is not formed. According to the reaction mechanism proposed by Tsuda et al.,[8c,8d] oxanickelacyclopentene **5** (Scheme 2) is also involved as a key intermediate in the catalytic cycle. The oxanickelacyclopentene leading to **7a** must possess an ethoxy group at the C atom adjacent to Ni. This means that not **5b** but **5a** is formed as the intermediate. These two examples clearly show that the regioselectivity of these coupling reactions is determined in the oxanickelacyclopentene formation step. Therefore, detailed knowledge of the oxanickelacyclopentene formation step is important in understanding these coupling reactions.

Not only from the chemistry of CO_2 fixation but also from a theoretical chemistry viewpoint, the formation of oxanickelacyclopentene is an attractive subject for research, because this reaction is considered to be sym-

#Present address: Department of Applied Chemistry, Faculty of Engineering, Kyushu Institute of Technology, Tobata, Kitakyushu 804.

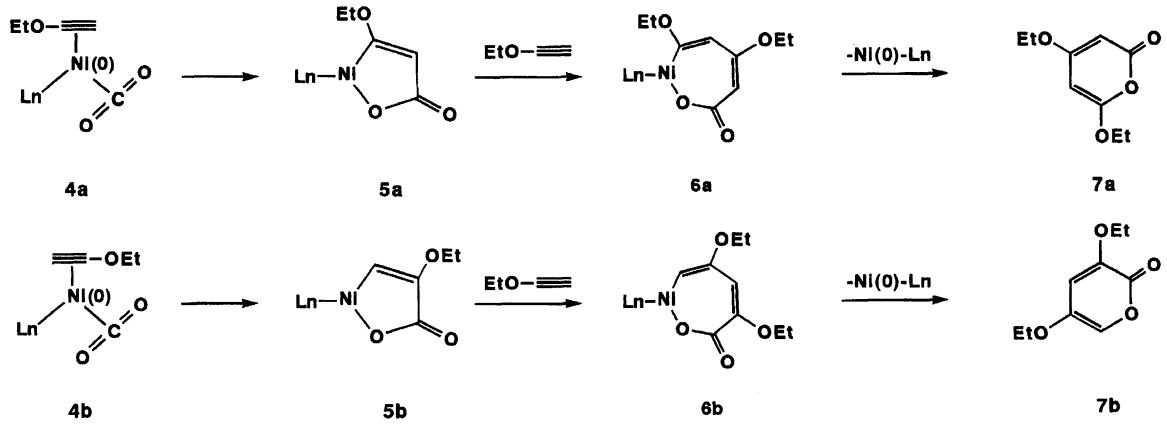

Scheme 2.

metry-forbidden in the absence of a transition metal complex.[11] In our previous report,[1] a theoretical investigation was carried out on the formation of oxanickelacyclopentene $[(H_3P)\overset{\frown}{Ni{-}CH{=}CH{-}CO}(O)]$ from CO_2, unsubstituted acetylene, and $[Ni(PH_3)]$ (Eq. 2). Although a detailed discussion has been presented on the

$$[Ni(PH_3)] + CO_2 + C_2H_2 \rightarrow [(H_3P)\overset{\frown}{Ni{-}CH{=}CH{-}CO}(O)] \quad (2)$$
8 **9**

catalytic function of Ni, the above-mentioned regioselectivity has not been examined at all. A similar coupling reaction of carbon dioxide with ethylene was also discussed by Dedieu et al., based on theoretical calculations of $[Ni(PH_3)_2(CO_2)]$ and $[Ni(PH_3)_2(C_2H_4)]$, in which the regioselectivity was also not discussed.[12]

In this work, the formation of oxanickelacyclopentene from CO_2, hydroxyacetylene, and $[Ni(PH_3)]$ is theoretically investigated with the ab initio MO/SD-CI method, where hydroxyacetylene is adopted here as a model of ethoxyacetylene. There are two oxanickelacyclopentene isomers, **9a** and **9b** produced by this reaction (Eq. 3); in **9a**, the OH group is introduced on the C atom adjacent to Ni, and in **9b**, the OH group is on the C atom apart from Ni. Our aims in this work are (1) to show

$$[Ni(PH_3)] + CO_2 + HC{\equiv}COH \rightarrow$$
8

$$[(H_3P)\overset{\frown}{Ni{-}C(OH){=}CH{-}CO}(O)]$$
9a

$$\text{or } [(H_3P)\overset{\frown}{Ni{-}CH{=}C(OH)CO}(O)] \quad (3)$$
9b

which oxanickelacyclopentene, **9a** or **9b**, is preferentially produced from carbon dioxide and hydroxyacetylene, (2) to clarify the reason for the regioselectivity, and (3) to make a detailed reactivity comparison between acetylene and hydroxyacetylene.

Calculations

Spin-restricted ab initio MO and limited SD-CI calculations were performed with Gaussian 86,[13a] 92,[13b] and MELD programs[14] respectively. Two kinds of basis sets were employed here. In the smaller one (BS-I), the core electrons of Ni (up to 3p) and P (up to 2p) were replaced with effective core potentials,[15,16] and their valence electrons were represented by (3s 2p 5d)/[2s 2p 2d][15] and (3s 3p)/[2s 2p][16] sets, respectively. MIDI-3 sets and a (4s)/[2s] set[17] were employed for C, O, and H respectively. In the larger basis set (BS-II), MIDI-4 sets were used for all the ligand atoms.[18] For Ni, Huzinaga's (13s 7p 5d) primitive set proposed for the $^3D(d^9s)$ state of Ni was augmented with a diffuse d primitive function (ζ=0.10)[19] and three p primitive functions whose exponents were taken to be the same as the three outermost s primitive functions of Ni. BS-I was used for geometry optimization at the Hartree–Fock (HF) level and BS-II for SD-CI calculations.

Limited SD-CI calculations were performed with a single HF configuration as a reference, where all of the core orbitals were excluded from the active space and virtual orbitals were transformed to K-orbitals[20] in order to improve the convergence of CI. All possible spin-adapted configuration functions were screened by using second-order Rayleigh–Schrödinger perturbation theory[21] to reduce the number of configuration functions on which variational SD-CI calculations were performed. The energy threshold adopted in the perturbation selection was 50 μhartree. The SD-excited configurations remaining after the perturbation selection included over 90% of the estimated SD correlation energy. The total energy obtained from the limited SD-CI calculation was corrected by estimating the correlation energy arising from the discarded SD excited configuration functions. Correction for the higher-order CI expansions was also made to estimate the total energy of a full CI calculation, to yield E_t(est. full CI). The reliability of the single reference (SR) SD-CI calculation

was ascertained in our previous work[1] on a similar reaction between unsubstituted C_2H_2 and carbon dioxide (Eq. 2), in which SR SD-CI calculations were compared with multi-reference SD-CI calculations. The MELD program was used for these SD-CI calculations.

The geometries of hydroxyacetylene, $C_2H(OH)$, and its Ni(O) complex, $[Ni(PH_3)\{C_2H(OH)\}]$, were optimized at the HF level with the energy gradient technique by using the Gaussian 86 and 92 programs. Geometry changes caused by the C_2H_2–CO_2 coupling reaction were optimized in our previous work[1] by taking the θ angle as a reaction coordinate (see Scheme 3 for the θ angle). Only the CC(OH) angle was optimized by least-squares fitting of the total energies, while the C–OH and O–H distances were taken from the optimized geometry of $[Ni(PH_3)\{C_2H(OH)\}]$ and the geometry of the other part was assumed to be the same as in the C_2H_2–CO_2 coupling reaction investigated previously.[1]

The OH-substituted C atom of $C_2H(OH)$ is called C^1 and the other C atom is C^2. Also, the C atom adjacent to Ni is named C^α and the C atom apart from Ni is C^β in this work.

We should mention here the reason that the model system is reasonable. Although the molar ratio of phosphine/Ni is 2 in many reaction conditions,[8] 2-pyrone is satisfactorily synthesized when the molar ratio is 1.[8a] We adopted the present model to mimic such conditions. A comparison between $[Ni(PH_3)(C_2H_2)(CO_2)]$ and $[Ni(PH_3)_2(C_2H_2)(CO_2)]$ was made in our previous work.[1]

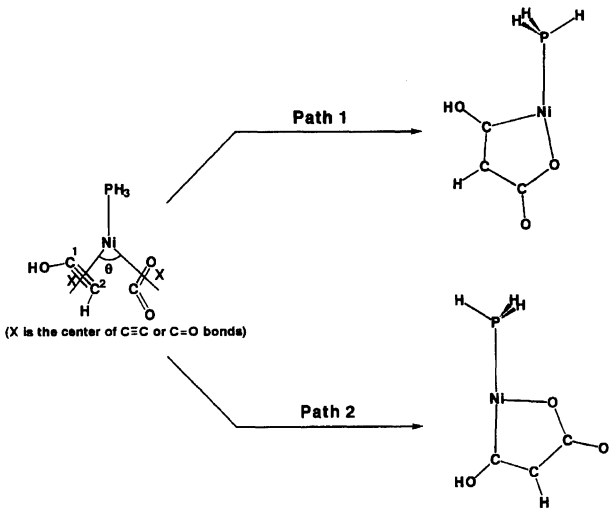

Scheme 3.

Results and Discussion

Comparison between $C_2H(OH)$ and C_2H_2. First, we investigated how the OH group influences the electronic structures of $C_2H(OH)$ and $[Ni(PH_3)\{C_2H(OH)\}]$. As shown in Fig. 1, the HF-optimized geometry of $[Ni(PH_3)\{C_2H(OH)\}]$ is non-linear (**10a** or **10c**). The geometry of **10b** was optimized at the HF-level under a constraint that the Ni–P bond and the Ni–X line were co-linear, where X was the center of the C≡C bond. Although **10b** is less stable than **10a** and **10c** at the HF-level, **10b** is more stable than **10a** and **10c** by 1.6 and 3.5 kcal mol^{-1}, respectively, at the SD-CI level (Table 1). From these results, it could be reasonably concluded that $[Ni(PH_3)\{C_2H(OH)\}]$ takes linear structure **10b**, like $[Ni(PH_3)(C_2H_2)]$ in which the linear structure is more stable than the non-linear one at the SD-CI level.[1]

A comparison between the equilibrium (linear) structures of $[Ni(PH_3)\{C_2H(OH)\}]$ and $[Ni(PH_3)(C_2H_2)]$ exhibits the following interesting features; (1) the Ni–C^1 and Ni–C^2 distances of the former are slightly shorter than those of the latter (R(Ni–C)=1.875 Å).[1] (2) The C≡C bond of the former is slightly longer than that of the latter (1.303 Å).[1] (3) The $C_2H(OH)$ part of $[Ni(PH_3)\{C_2H(OH)\}]$ distorts to an extent similar to the C_2H_2 part in $[Ni(PH_3)(C_2H_2)]$ (see the CCH angle). And, (4) the Ni–C^2 distance is shorter than the Ni–C^1

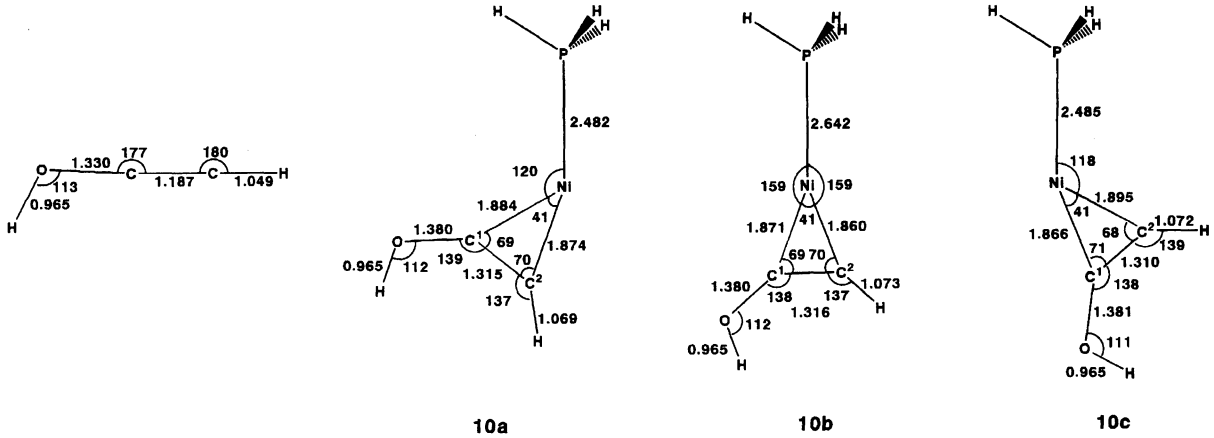

Fig. 1. Optimized geometries of $C_2H(OH)$ and $[Ni(PH_3)\{C_2H(OH)\}]$.[a] Bond length in Å and bond angle in degree.
a) **10b** was optimized under assumption that the Ni–PH_3 bond and the Ni–X line were collinear, where X was the center of the C–C bond.

Table 1. Mulliken Populations of C_2H_2, $C_2H(OH)$, and Their Ni(O) Complexes

	C_2H_2	$C_2H(OH)$	$[Ni(PH_3)(C_2H_2)]$[a]	$[Ni(PH_3)\{C_2H(OH)\}]$[b]		
				10a	**10b**	**10c**
Ni			27.291	27.291	27.265	27.278
PH_3			17.893	17.852	17.869	17.857
C^1	6.331	6.030	6.572	6.124	6.188	6.208
C^2	6.331	6.173	6.572	6.659	6.630	6.553
Δq[c]	0.0	0.0	0.816	0.883	0.911	0.865
ΔE (kcal mol^{-1})[d]				1.6	0.0	3.5

a) The linear structure. b) See Fig. 1 for **10a**, **10b**, and **10c**. c) The increase in electron population of C_2H_2 or $C_2H(OH)$ upon coordination to Ni. d) Relative energy at the SD-CI level.

distance in $[Ni(PH_3)\{C_2H(OH)\}]$.

The above results can be explained in terms of the π^* orbitals of C_2H_2 and $C_2H(OH)$ which play an important role in the acetylene coordination to such a low valent transition metal as Ni(O).[23] Although the π^* orbital of $C_2H(OH)$ lies at almost the same energy level as that of C_2H_2 in their equilibrium structures, the former becomes much more stable in terms of energy than the latter upon undergoing the bending distortion, as shown in Fig. 2. This means that although C_2H_2 and $C_2H(OH)$ distort to a similar extent in $[Ni(PH_3)L]$ ($L=C_2H_2$ of $C_2H(OH)$), the π^* orbital of $C_2H(OH)$ lies at a lower energy than that of C_2H_2. As a result, the π back-donation from the $d\pi$ orbital of Ni to the π^* orbital of $C_2H(OH)$ is stronger in $[Ni(PH_3)\{C_2H(OH)\}]$ than in $[Ni(PH_3)(C_2H_2)]$. This strong back-donation in $[Ni(PH_3)\{C_2H(OH)\}]$ increases the electron population of $C_2H(OH)$ and decreases the Ni atomic population to a greater extent than in $[Ni(PH_3)(C_2H_2)]$, which facilitates the electron donation from PH_3 to Ni in the former. These features are certainly observed in the Mulliken population (Table 1).

The other important result is that the C^1 atomic population changes very little but the C^2 atomic population significantly increases upon coordination of $C_2H(OH)$ with $[Ni(PH_3)]$. This electron redistribution is interpreted in terms of the π^* orbital of $C_2H(OH)$. As shown in Fig. 3, this π^* orbital expands more largely on the C^2 atom than on the C^1 atom. Consequently, the Ni–C^2 interaction is stronger than the Ni–C^1 interaction, and the C^2 atomic population increases more than the C^1 atomic population upon coordination of $C_2H(OH)$ with Ni. Thus, it is concluded that the shape of the π^* orbital of $C_2H(OH)$ results in a shorter Ni–C^2 distance than the Ni–C^1 distance. This feature of the π^* orbital is also related to the regioselectivity observed in the Ni(O)-catalyzed coupling reaction between CO_2 and $C_2H(OH)$, as will be discussed below.

Changes in Geometry and Energy Upon Oxanickelacyclopentene Formation from $[Ni(PH_3)]$, $C_2H(OH)$, and CO_2. In the reaction of unsubstituted acetylene with $[Ni(PH_3)]$ and CO_2, there are two possible reaction pathways (see Scheme 3); in one (path 1), PH_3 moves to the trans-position of the O atom, and in the other (path 2), PH_3 moves to the trans-position of the C atom. Because path 1 leads to a

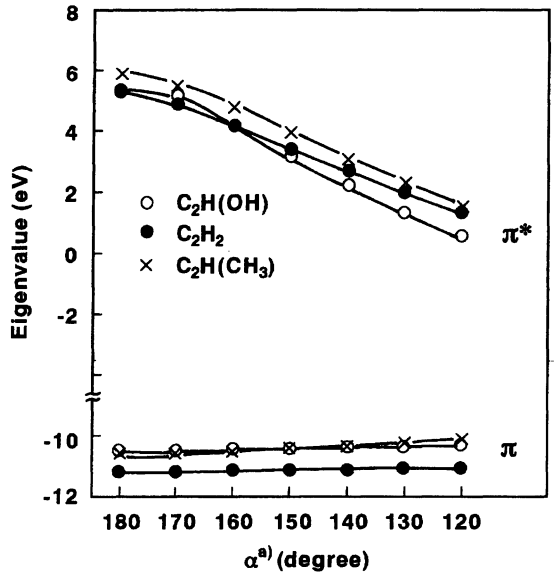

Fig. 2. Energy levels of the π^* orbitals[b] of C_2H_2, $C_2H(OH)$ and $C_2H(CH_3)$. a) The CCH, CC(OH) or $CC(CH_3)$ angle. b) Only π and π^* orbitals in the molecular plane are given.

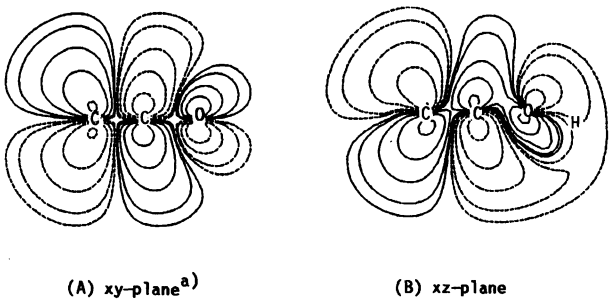

Fig. 3. Contour maps of the π^* orbital of $C_2H(OH)$.[a] a) The OH group lies on the xz-plane. Contour values; ±0.2, ±0.1, ±0.05, ±0.02, ±0.01.

more stable product with a lower activation energy than does path 2,[1] the effects of the substituent OH on path 1 were investigated. The reaction course is called path 1a when OH is introduced on the C^{α} atom, and path 1b when OH is introduced on the C^{β} atom. Several important geometries along paths 1a and 1b are shown in Fig. 4. At the early stage of the reaction, CO_2 distorts only slightly, but $C_2H(OH)$ distorts considerably in [Ni(PH$_3$){C$_2$H(OH)}(CO$_2$)] (see **11a** and **11b** in Fig. 4). This result suggests that $C_2H(OH)$ coordinates strongly to Ni(O) but CO_2 interacts only weakly with Ni(O). In fact, the coordinate bond of $C_2H(OH)$ was estimated to be 16 kcal mol^{-1} stronger than that of CO_2 from the following assumed reaction;

$$[Ni(PH_3)\{C_2H(OH)\}]+CO_2 \rightarrow [Ni(PH_3)(CO_2)]+C_2H(OH) \quad (4)$$

where the left-hand side of this equation is about 16 kcal mol^{-1} more stable than the right-hand side at the SD-CI level. The above results indicate that $C_2H(OH)$ coordinates first to [Ni(PH$_3$)], yielding [Ni(PH$_3$){C$_2$H(OH)}], and then CO_2 approaches [Ni(PH$_3$){C$_2$H(OH)}].[24] As the reaction proceeds, the CC(OH) angle becomes smaller as expected,[25] because the C^1 and C^2 atoms are becoming sp^2 hybridized in the reaction.[26]

Apparently, as shown in Fig. 5 and Table 2, the $C_2H(OH)$–CO_2 coupling reaction occurs through path 1a with a slightly lower activation energy (E_a) of 27 kcal mol^{-1} than the E_a (30 kcal mol^{-1}) of the unsubstituted C_2H_2–CO_2 coupling reaction.[1] On the other hand, the reaction proceeds through path 1b with a higher E_a of 38 kcal mol^{-1} than the E_a of the C_2H_2–CO_2 coupling reaction. These results clearly show that the

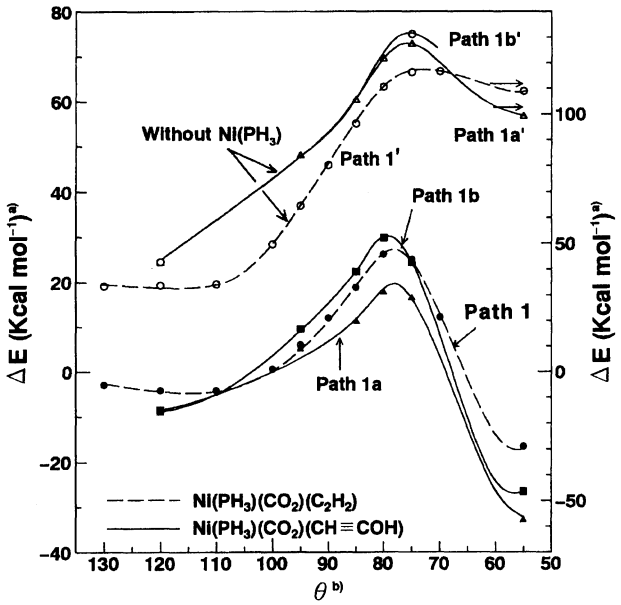

Fig. 5. Energy changes[a] by the oxanickelacyclopentene formation from [Ni(PH$_3$)], CO_2, and $C_2H(OH)$. a) Energy zero is taken for the infinite separation between [Ni(PH$_3$){C$_2$H(OH)}] and CO_2.

OH group on C^{α} accelerates the coupling reaction, but that the OH group on C^{β} suppresses the reaction. Furthermore, path 1a leads to the more stable product **9a**, but **1b** leads to the less stable **9b**, as shown in Fig. 5. Consequently, **9a** is formed in preference to **9b**. These results are consistent with the experimentally-reported regioselectivity in the Ni(O)-catalyzed coupling reaction between ethoxyacetylene and CO_2,[8c] in which 4,6-diethoxy-2-pyrone is formed. This product can be pro-

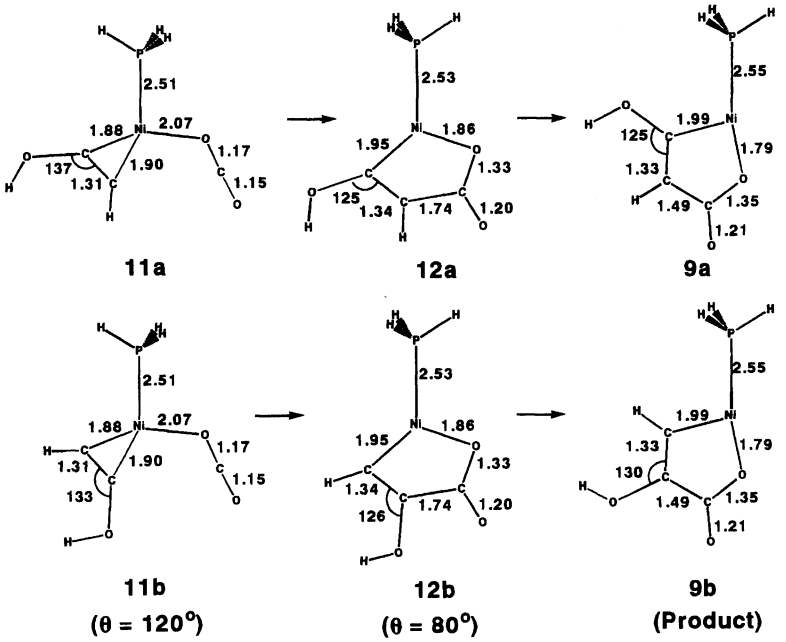

Fig. 4. Several important geometries along the formation reaction of oxanickelacyclopentene from [Ni(PH$_3$)], CO_2, and $C_2H(OH)$. Bond length in Å and bond angle in degree.

Table 2. Activation Energies (E_a) and Reaction Energies (ΔE) of the CO_2 Coupling Reaction with Acetylene (kcal mol^{-1} at SD-CI Level after Davidson–Silver Correction)

	CO_2–C_2H_2	CO_2–$C_2H(OH)$	
	path 1	path 1a	path 1b
E_a[b)]	30	27	38
ΔE[c)]	−17	−31	−25

a) kcal mol^{-1} at the SD-CI level. b) The energy difference between **12** (θ=80°) and **11** (θ=120°) (see Fig. 5 for **11** and **12**). c) The energy difference between the product and the reactant in which Ni and CO_2 are infinitely separate. A negative value means the exothermicity.

duced not from oxanickelacyclopentene **5b** possessing the ethoxy group on the C^β atom, but from **5a** possessing the ethoxy group on the C^α atom,[8c)] as shown in Scheme 2. This geometry of **5a** agrees with **9a**. Also, the E_a value of path 1a is lower than the E_a value of the unsubstituted C_2H_2–CO_2 coupling reaction, which is consistent with the experimental finding that ethoxyacetylene is more reactive than alkyl-substituted acetylene[8c)] (see below for a more detailed discussion).

The energy changes of the $C_2H(OH)$–CO_2 and C_2H_2–CO_2 coupling reactions without [Ni(PH_3)] are shown in Fig. 5, to clarify the role of [Ni(PH_3)], where the geometries of the $C_2H(OH)$–CO_2 and C_2H_2–CO_2 systems are taken to be the same as those in paths 1a, 1b, and 1, respectively, and only [Ni(PH_3)] is eliminated from the reaction system without any other modification. The reaction paths in the absence of [Ni(PH_3)] are described as paths 1a′, 1b′, and 1′, which correspond to paths 1a, 1b, and 1, respectively. Several interesting features are observed in these uncatalyzed reactions; (1) the $C_2H(OH)$–CO_2 coupling reaction causes greater energy destabilization than the C_2H_2–CO_2 coupling reaction, (2) path 1a′ is slightly more stable in terms of energy than path 1b′ around the transition state (TS), and (3) around the TS, the energy difference between paths 1a′ and 1b′ is much smaller than that between paths 1a and 1b. These features lead to the conclusion that $C_2H(OH)$ is more reactive than C_2H_2 only when [Ni(PH_3)] exists in the reaction system, and [Ni(PH_3)] enhances the regioselectivity of the $C_2H(OH)$–CO_2 coupling reaction.

Factors Determining the Regioselectivity and the Reactivity. **9a** would be more easily formed than **9b** if CO_2 more easily approaches [Ni(PH_3){$C_2H(OH)$}] **10b** from the right-hand side than from the left-hand side (see Fig. 1). As is clearly shown in Fig. 5, however, the energy difference between paths 1a and 1b is very small at the early stage of the reaction, but significantly large (11 kcal mol^{-1}) at the TS. This means that the regioselectivity is not determined at the step where CO_2 approaches [Ni(PH_3){$C_2H(OH)$}]. The energy difference between products **9a** and **9b** is also much smaller than the energy difference at the TS between paths 1a and 1b. Thus, the regioselectivity of this reaction is determined at the TS, and therefore, the bonding nature and electronic structure of the TS should be investigated in detail to clarify the factors determining the regioselectivity.

Before starting this detailed discussion, we summarize here our previous findings on Ni(O) catalysis.[1)] When [Ni(PH_3)] does not exist in the reaction system, HOMO ϕ_2 of the C_2H_2–CO_2 system mainly involves an anti-bonding overlap between the π orbitals of CO_2 and C_2H_2, as shown in Scheme 4. When [Ni(PH_3)] exists in the reaction system, the Ni dσ orbital overlaps well with LUMO ϕ_3 in a bonding way, to yield a charge-transfer (CT) interaction from the Ni dσ orbital to LUMO ϕ_3. Because LUMO ϕ_3 involves a bonding interaction between the π^* orbitals of CO_2 and C_2H_2, this CT interaction stabilizes the TS and accelerates the C–C bond formation between C_2H_2 and CO_2. Thus, it has been reasonably concluded that the catalytic function of Ni(O) arises from this CT interaction. To ascertain that the $C_2H(OH)$–CO_2 reaction system has a HOMO similar to that of the C_2H_2–CO_2 reaction system, the HOMO character was examined around the TS by drawing a contour map. This contour map (Fig. 6) is essentially the same as the HOMO previously observed in the C_2H_2–CO_2 coupling reaction;[1)] the π^* orbital of CO_2 overlaps with the π^* orbital of $C_2H(OH)$ in a bonding way, and the Ni dσ orbital contributes to this HOMO only a little as in our previous results, which indicates that the charge-transfer has already occurred around the TS.

Now, we will examine how the OH group influences this CT interaction at the TS. In reaction path 1a, CO_2 approaches the C^2 atom of $C_2H(OH)$, while in path 1b, CO_2 approaches the C^1 atom. Because the π^* orbital of $C_2H(OH)$ expands more on the C^2 atom than on the C^1 atom (Fig. 3), the π^*–π^* bonding overlap between CO_2 and $C_2H(OH)$ is greater in path 1a than in path 1b; accordingly, LUMO ϕ_3 lies at a lower energy in path 1a than in path 1b. Thus, the occupied dσ orbital

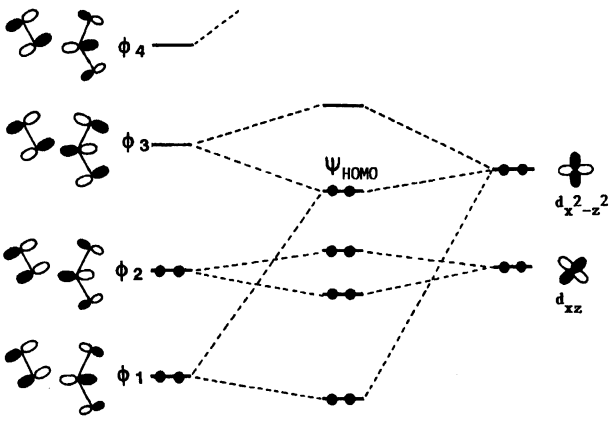

Scheme 4.

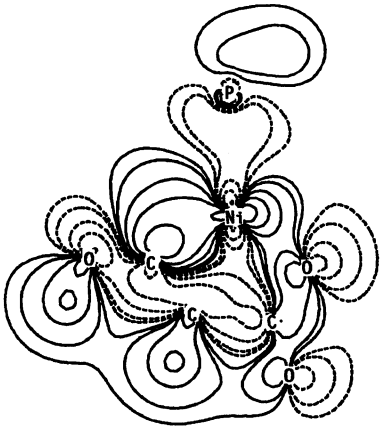

Fig. 6. Contour map[a] of HOMO of [Ni(PH$_3$){C$_2$H(OH)}(CO$_2$)] **12a** in the path 1a. a) Contour values; ±0.2, ±0.1, ±0.05, ±0.02, ±0.01.

of [Ni(PH$_3$)] can form a stronger CT interaction with ϕ_3 in path 1a than in path 1b, which better stabilizes the TS and accelerates the C–C bond formation between C$_2$H(OH) and CO$_2$ more in path 1a than in path 1b. Next, C$_2$H(OH) will be compared with C$_2$H$_2$. The π^*–π^* bonding overlap between C$_2$H(OH) and CO$_2$ is larger than that between C$_2$H$_2$ and CO$_2$, since the π^* orbital of C$_2$H(OH) lies at a lower energy than that of C$_2$H$_2$ (Fig. 3) (consider that the π^* orbital of CO$_2$ lies at a lower energy than those of C$_2$H(OH) and C$_2$H$_2$). As a result, the CT interaction from the Ni dσ orbital to the π^*–π^* bonding overlap is stronger in the C$_2$H(OH)–CO$_2$ coupling reaction (path 1a)[26] than in the C$_2$H$_2$–CO$_2$ coupling reaction (path 1), which leads to a more stable TS and a stronger bonding interaction between C$_2$H(OH) and CO$_2$ in path 1a than in path 1. In fact, the HOMO of path 1a is more stable in energy than that of path 1b around the TS; at $\theta=80°$, ϵ(HOMO)$=-10.9$ eV in path 1a, -10.4 eV in path 1b,[27] and -10.3 eV in path 1. Although the HOMO of path 1b lies at an energy level similar to that of path 1, path 1b requires a higher E_a than path 1. This is because other factors such as electrostatic interaction are less favorable in path 1b than in path 1, as will be discussed below.

The electrostatic interaction is expected to play some role in determining the regioselectivity. Because the C atom of CO$_2$ is positively charged, electrostatic stabilization occurs when CO$_2$ approaches the negatively charged atom. As shown in Table 1, the C^2 atom is more negatively charged than the C^1 atom in C$_2$H(OH). This electron distribution makes path 1a more favorable than path 1b. The electron distribution of C$_2$H(OH) is not, however, responsible for the higher reactivity of C$_2$H(OH) than that of C$_2$H$_2$, because the C^1 and C^2 atoms of C$_2$H(OH) are less negatively charged than the C atom of C$_2$H$_2$. The situation significantly changes on going to [Ni(PH$_3$){C$_2$H(OH)}] in which the C^1 atom is less negatively charged but the C^2 atom is more negatively charged than the C atom in [Ni(PH$_3$)(C$_2$H$_2$)] (see Table 1). When the C atom of CO$_2$ approaches the less negatively charged C^1 atom of C$_2$H(OH) (path 1b), the coulombic interaction between C$_2$H(OH) and CO$_2$ is less attractive than that between C$_2$H$_2$ and CO$_2$ (path 1). On the other hand, when the C atom of CO$_2$ approaches the C^2 atom of C$_2$H(OH) (path 1a), the coulombic interaction between C$_2$H(OH) and CO$_2$ becomes more attractive than that between C$_2$H$_2$ and CO$_2$ (path 1). Thus, the electrostatic stabilizing energy is the greatest in path 1a, lower in path 1, and the least in path 1b, which also contributes to the increasing order of Ea, path 1a<path 1<path 1b.

In conclusion, the regioselectivity of this reaction and the higher reactivity of hydroxyacetylene arise from the π^* orbital of C$_2$H(OH) and the electron distribution of [Ni(PH$_3$){C$_2$H(OH)}].

Finally, we mention the reactivity of methyacetylene C$_2$H(CH$_3$) because alkyl-substituted acetylene is used as a substrate of Ni-catalyzed acrylic acid synthesis from CO$_2$. From the above discussion, we can predict that an acetylene derivative is a good substrate for this kind of coupling reaction when its π^* orbital lies at a low energy level. The π^* orbital of methylacetylene lies at a higher energy level than those of C$_2$H$_2$ and C$_2$H(OH) in both equilibrium and distorted structures (Fig. 2), probably because of the electron-donating methyl group. This suggests that the C$_2$H(CH$_3$)–CO$_2$ coupling reaction would require a higher E_a than the C$_2$H(OH)–CO$_2$ coupling reaction. Thus, it is reasonably expected that use of ethoxyacetylene as a substrate would lead to higher yields of the acrylic acid derivative in the Ni-catalyzed electrochemical coupling reaction of CO$_2$ (Eq. 2).

The regioselectivity of the C$_2$H(CH$_3$)–CO$_2$ coupling reaction is also noteworthy. As described above, the preferential formation of **1** (considering Eq. 1) means that oxanickelacyclopentene **3a** is more easily formed than **3b** in the Ni(bpy)-catalyzed coupling reaction.[7] This regioselectivity is opposite those in the Ni(phosphine)-catalyzed C$_2$H(OH)–CO$_2$ and C$_2$H(R)–CO$_2$ coupling reactions.[8c] Since C$_2$H(CH$_3$) has an electron distribution and π^* orbitals similar to those of C$_2$H(OH),[29] the different selectivity of Eq. 1 would be attributed not to the interaction between C$_2$H(CH$_3$) and CO$_2$, but to the interaction between C$_2$H(CH$_3$) and Ni(bpy). We calculated Ni (II)–vinyl complexes, [NiL(PH$_3$)(CX=CH$_2$)] **13a** and [NiL(PH$_3$)(CH=CHX)] **13b** (L=H or PH$_3$; X=OH or CH$_3$), to investigate the substituent effects on the stability of the Ni(II)–vinyl bond (Scheme 5). Their geometries were optimized at the HF/BS-I level,[31] and the relative stabilities were estimated at the SD-CI/BS-II level. Interestingly, the relative stabilities depend on the ligand (Table 3): When L is the small H (hydride) ligand, **13a** is more stable than **13b** for both X=CH$_3$ and OH. On the other hand, when L is the larger PH$_3$ ligand, **13a** (X=CH$_3$) is less

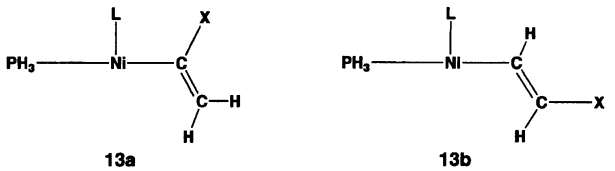

Scheme 5.

Table 3. Relative Stabilities[a] of [NiL(PH$_3$)(CX=CH$_2$)] **13a** and [NiL(PH$_3$)(CH=CHX)] **13b** (L=H or PH$_3$; X=CH$_3$ or OH)

	L=H		L=PH$_3$	
	X=CH$_3$	X=OH	X=CH$_3$	X=OH
ΔE[b]	2.4	2.5	−16.0	9.9

a) SD-CI/BS-II calculation. b) $\Delta E = E_t(\mathbf{13a}) - E_t(\mathbf{13b})$. A positive value represents that **13b** is more stable than **13a** (vice versa).

stable than **13b** (X=CH$_3$), while **13a** (X=OH) is still more stable than **13b** (X=OH). If electronic factors are important, the relative stabilities of **13a** (X=CH$_3$) and **13b** (X=CH$_3$) would not be different between L=H and L=PH$_3$ like the relative stabilities for X=OH. One of the plausible explanations is that electronic factors are important for X=OH and that steric repulsion becomes important for X=CH$_3$ when a bulky ligand exists at the cis-position of the vinyl group.[32] Moreover, the steric repulsion between the ligand and the alkyl substituent is much larger in the real substrate than in model system **13a** (X=CH$_3$) because C$_2$H(C$_6$H$_{13}$) is used as a substrate.[7] In **3b**, the bpy ligand would give rise to steric repulsion with the C$_6$H$_{13}$ substituent, which would lead to the preferential formation of **3a**. In the Ni(phosphine)-catalyzed coupling reaction, one phosphine tends to be eliminated from Ni at the TS even when the system involves two phosphines per Ni.[1] This means that the selectivity at the TS would be similar to that of a mono-phosphine system;[33] i.e., the α-alkyl-substituted vinyl complex is more stable than the β-substituted one. Thus, C$_2$H(R) exhibits the same regioselectivity as that of C$_2$H(OH) in the Ni(phosphine) catalytic reaction.

Concluding Remarks.

The formation reaction of oxanickelacyclopentene [(H$_3$P)Ni–C(OH)=CHCO(O)] **9a** and [(H$_3$P)Ni–CH=C–(OH)CO(O)] **9b** from [Ni(PH$_3$)], CO$_2$, and hydroxyacetylene, C$_2$H(OH) (a model of ethoxyacetylene), was theoretically investigated with the *ab initio* MO/SD-CI method. **9a** is yielded with a lower E_a value of 27 kcal mol^{-1} and a higher E_{exo} value of 31 kcal mol^{-1} than those of **9b** (E_a = 38 kcal mol^{-1} and E_{exo} = 25 kcal mol^{-1}). This preferential formation of **9a** is in accord with the selective formation of 4,6-diethoxy-2-pyrone in the Ni(O)-catalyzed coupling reaction between CO$_2$ and ethoxyacetylene. The lower E_a for **9a** formation agrees with the experimental finding that the yields of 4,6-diethoxy-2-pyrone are higher than those of 4,6-dialkyl-2-pyrone. These results are interpreted in terms of the π^* orbital of C$_2$H(OH). The catalytic function of Ni(O) is attributed to the CT interaction from the occupied dσ orbital of Ni to the π^*–π^* bonding overlap between CO$_2$ and C$_2$H(OH). This π^*–π^* bonding interaction lies at a lower energy level in path 1a than in path 1b, because the π^* orbital of C$_2$H(OH) expands more on the C^2 atom than on the C^1 atom. As a result, the CT interaction from the occupied dσ orbital of Ni to the π^*–π^* bonding overlap is stronger in path 1a than in path 1b. The higher reactivity of C$_2$H(OH) than that of C$_2$H$_2$ is also interpreted in terms of this CT interaction; because the distorted C$_2$H(OH) has a π^* orbital at a lower energy than that of the distorted C$_2$H$_2$, C$_2$H(OH) can form a greater π^*–π^* bonding overlap with CO$_2$ than does C$_2$H$_2$ (remember that the coupling reaction causes the bending distortion of C$_2$H$_2$ and C$_2$H(OH)). Accordingly, the C$_2$H(OH)–CO$_2$ reaction system (path 1a) involves a stronger CT interaction from the dσ orbital of Ni(PH$_3$) to this π^*–π^* bonding overlap than the C$_2$H$_2$–CO$_2$ reaction system. Furthermore, the positively charged C atom of CO$_2$ yields the most attractive electrostatic interaction with the C^2 atom of [Ni(PH$_3$){C$_2$H(OH)}], the next attractive one with the C atom of [Ni(PH$_3$)(C$_2$H$_2$)], and the least attractive one with the C^1 atom of [Ni(PH$_3$){C$_2$H(OH)}], because C^2 of [Ni(PH$_3$){C$_2$H(OH)}] is the most, C of [Ni(PH$_3$)(C$_2$H$_2$)] is the next, and C^1 of [Ni(PH$_3$){C$_2$H(OH)}] is the least negatively charged. Because of all these factors, **9a** is formed in preference to **9b**, and the reactivity of C$_2$H(OH) is higher than that of C$_2$H$_2$. From this discussion, we can predict that the acetylene derivative possessing a π^* orbital at a low energy level should be used as a substrate to effectively perform this kind of coupling reaction with CO$_2$. Interestingly, the regioselectivity of the Ni(bpy)-catalyzed C$_2$H(C$_6$H$_{13}$)–CO$_2$ coupling[7] is opposite that of the Ni(phosphine)-catalyzed C$_2$H(OH)–CO$_2$ coupling.[8c] This different selectivity of the C$_2$H(C$_6$H$_{13}$)–CO$_2$ coupling is interpreted in terms of the steric repulsion between bpy and *n*-C$_6$H$_{13}$ in oxanickelacyclopentene.

The authors thank Professor T. Tsuda (Kyoto University) for his instructive suggestions on the high reactivity of ethoxyacetylene. This work was financially supported in part by the Ministry of Education, Culture, and Science (Grant-in Aids No. 04243102 and No. 06227256). Calculations were carried out with Hitachi S-820 and M-680 Computers at the Institute for Molecular Science (Okazaki, Japan).

References

1) Part 1: S. Sakaki, K. Mine, D. Taguchi, and T. Arai, *Bull. Chem. Soc. Jpn.*, **66**, 3289 (1993).

2) For instance: a) D. Walther, *Coord. Chem. Rev.*, **79**, 135 (1987); b) A. Behr, *Angew. Chem., Int. Ed. Engl.*, **27**, 661 (1988); c) P. Braunstein, D. Matt, and D. Nobel, *Chem. Rev.*, **88**, 747 (1988); d) A. R. Culter, P. K. Hanna, and J. C. Vites, *Chem. Rev.*, **88**, 1363 (1988); e) H. Werner, *Angew. Chem., Int. Ed. Engl.*, **29**, 1077 (1990).

3) a) Y. Sasaki, Y. Inoue, and H. Hashimoto, *J. Chem. Soc., Chem. Commun.*, **1976**, 605. b) Y. Inoue, Y. Itoh, H. Kazama, and H. Hashimoto, *Bull. Chem. Soc. Jpn.*, **53**, 3329 (1980).

4) a) A. Behr, R. He, K. -D. Juszak, C. Krüger, and Y. -H. Tsay, *Chem. Ber.*, **119**, 991 (1986); b) A. Behr and K. -D. Juszak, *J. Organomet. Chem.*, **225**, 263 (1983); c) A. Behr and U. Kanne, *J. Organomet. Chem.*, **317**, C41 (1986).

5) a) G. Burkhart and H. Hoberg, *Angew. Chem., Int. Ed. Engl.*, **21**, 76 (1982); b) H. Hoberg, D. Schaefer, G. Burkhart, C. Krüger, and M. J. Romao, *J. Organomet. Chem.*, **266**, 203 (1984); c) H. Hoberg, S. Gross, and A. Milchereit, *Angew. Chem., Int. Ed. Engl.*, **26**, 571 (1987); d) H. Hoberg, Y. Peres, A. Milchereit, and S. Gross, *J. Organomet. Chem.*, **345**, C17 (1988); e) H. Hoberg and D. Bärhausen, *J. Organomet. Chem.*, **379**, C7 (1989).

6) D. Walther, H. Schönberg, E. Dinjus, and J. Sieler, *J. Organomet. Chem.*, **334**, 377 (1987).

7) a) E. Duñach and J. Périchon, *J. Organomet. Chem.*, **352**, 239 (1988); b) E. Duñach, S. Dérien, and J. Périchon, *J. Organomet. Chem.*, **364**, C33 (1989); c) S. Dérien, J. C. Clinet, E. Duñach, and J. Périchon, *J. Chem. Soc., Chem. Commun.*, **1991**, 549; d) S. Dérien, E. Duñach, and J. Périchon, *J. Am. Chem. Soc.*, **113**, 8447 (1991).

8) a) T. Tsuda, S. Morikawa, R. Sumiya, and T. Saegusa, *J. Org. Chem.*, **53**, 3140 (1988); b) T. Tsuda, S. Morikawa, and T. Saegusa, *J. Chem. Soc., Chem. Commun.*, **1989**, 9; c) T. Tsuda, K. Kunisada, N. Nagahara, S. Morikawa, and T. Saegusa, *Synth. Commun.*, **19**, 1575 (1989); **20**, 313 (1990); d) T. Tsuda, S. Morikawa, N. Hasegawa, and T. Saegusa, *J. Org. Chem.*, **55**, 2978 (1990).

9) P. Braunstein, D. Matt, and D. Nobel, *J. Am. Chem. Soc.*, **110**, 3207 (1988).

10) R. Mahé, Y. Sasaki, C. Bruneau, and D. H. Dixneuf, *J. Org. Chem.*, **54**, 1518 (1989).

11) a) A. Stockis and R. Hoffmann, *J. Am. Chem. Soc.*, **102**, 2952 (1980); b) R. J. McKinney, D. L. Thorn, R. Hoffmann, and A. Stockis, *J. Am. Chem. Soc.*, **103**, 2595 (1981).

12) a) A. Dedieu and F. Ingold, *Angew. Chem., Int. Ed. Engl.*, **28**, 1694 (1989); b) C. Jegat, M. Fouassier, M. Tranquille, J. Mascetti, I. Tommasi, M. Aresta, F. Ingold, and A. Dedieu, *Inorg. Chem.*, **32**, 1279 (1993); c) A. Dedieu, D. Bo, and F. Ingold, "Enzeime Model Carboxylation Reduction Reaction, Carbon Dioxide Utilization," NATO ASI Ser. C, Reidle, Dordrecht (1990), p.23.

13) a) M. J. Frisch, J. S. Binkley, H. B. Schlegel, K. Raghavachari, C. F. Melius, R. Martin, J. J. P. Stewart, F. W. Bobrowicz, C. M. Rohlfing, L. R. Kahn, D. J. DeFrees, R. Seegar, R. A. Whiteside, D. J. Fox, E. M. Fluder, and J. A. Pople, "Gaussian 86," Carnegie-Mellon Quantum Chemistry Publishing Unit, Pittsburgh, PA (1986); b) M. J. Frisch, G. W. Trucks, M. Head-Gordor, P. M. W. Gill, M. W. Wong, J. B. Foresman, B. G. Johnson, H. B. Schlegel, M. A. Robb, E. S. Replogle, R. Gomperts, J. L. Andres, K. Raghavachari, J. S. Binkley, C. Gonzalez, R. L. Martin, D. J. Fox, D. J. DeFrees, J. Baker, J. J. P. Stewart, and J. A. Pople, "Gaussian 92," Gaussian, Inc., Pittsburgh, PA (1992).

14) E. R. Davidson, L. McMurchie, S. Elbert, S. R. Langhoff, D. Rawlings, and D. Feller, "MELD," IMS Computer Center Library, No. 030, University of Washington, Seattle, WA.

15) P. J. Hay and W. R. Wadt, *J. Chem. Phys.*, **82**, 270 (1985).

16) W. R. Wadt and P. J. Hay, *J. Chem. Phys.*, **82**, 284 (1985).

17) T. H. Dunning and P. J. Hay, "Gaussian Basis Sets for Molecular Calculation," in "Methods of Electronic Structure Theory," ed by H. F. Schaefer, Plenum, New York (1977), p.1.

18) S. Huzinaga, J. Andzelm, M. Klobukowski, E. Radzio-Andzelm, Y. Sakai, and H. Tatewaki, "Gaussian Basis Sets for Molecular Calculations," Elsevier, Amsterdam (1984).

19) This exponent was determined by the even-tempered criterion.

20) D. Feller and E. R. Davidson, *J. Chem. Phys.*, **74**, 3997 (1981).

21) S. R. Langhoff and E. R. Davidson, *Int. J. Quantum Chem.*, **8**, 61 (1974).

22) E. R. Davidson and D. W. Silver, *Chem. Phys. Lett.*, **52**, 403 (1977).

23) a) K. Kitaura, S. Sakaki, and K. Morokuma, *Inorg. Chem.*, **20**, 2292 (1981); b) S. Sakaki, K. Kitaura, and K. Morokuma, *Inorg. Chem.*, **21**, 760 (1982); c) S. Sakaki, N. Koga, and K. Morokuma, *Inorg. Chem.*, **29**, 3110 (1990).

24) Dedieu et al. proposed a different feature on the reaction in which $[Ni(PH_3)_2(CO_2)]$ is first formed and then C_2H_2 approaches it.[12] The difference between their feature and ours would arise from the defference in a model employed, which has been discussed in our previous work.[1]

25) Only one exception is observed in the CC(OH) angle of **12b** (θ=80°) along the path 1b. This angle is smaller than that in the product **9b**. The reason would be steric repulsion between H and OH; because the HCC angle becomes smaller in the product, which would allow the CC(OH) angle open. In the path 1a, the OH group causes steric repulsion with both the H atom and PH_3; accordingly, the CC(OH) angle little changes upon going to the product.

26) The C atom takes the sp hybridization in $C_2H(OH)$, but the p character increases upon coordination of $C_2H(OH)$ to $[Ni(PH_3)_2]$ as clearly shown by the geometry of $[Ni(PH_3)\{C_2H(OH)\}]$ **10a**, **10b**, and **10c**. However, the hybridization of the C atom does not reach the complete sp^2 hybridization even in $[Ni(PH_3)\{C_2H(OH)\}]$.

27) It is not easy to compare the $C_2H(OH)$–CO_2 coupling reaction of path 1b with the C_2H_2–CO_2 coupling reaction, because the π^*–π^* bonding overlap in the path 1b would be smaller than that in the C_2H_2–CO_2 coupling reaction (remember that CO_2 approaches C^1 of $C_2H(OH)$ in the path 1b and the π^* orbital of $C_2H(OH)$ less expands on the C^1

atom than on the C^2 atom).

28) The HOMO contour map of the path 1a exhibits a slightly larger C–C bonding overlap between CO_2 and C_2H-(OH) than that of the path 1b. However, the difference between paths 1a and 1b is not significant; the contour of 0.1 in the former covers only slightly larger area than in the latter, while the other difference is not observed clearly. Therefore, the HOMO contour map of the path 1b is omitted here.

29) E. Nakamura, Y. Miyachi, N. Koga, and K. Morokuma, *J. Am. Chem. Soc.*, **114**, 6686 (1992).

30) CH_3 and OH were placed as shown in Scheme 5 to mimic their positions in oxanickelacyclopentene.

31) Important geometrical parameters are as follows (bond length in Å and bond angle in degree): Where L is H and X is CH_3, R(Ni–H)=1.537, R(Ni–P)=2.616, R(Ni–C)=1.945, R(C=C)=1.331, ∠HNiP=95, ∠HNiC=102, and ∠NiCMe=125 for **10a**; R(Ni–H)=1.534, R(Ni–P)=2.619, R(Ni–C)=1.951, R(C=C)=1.331, ∠HNiP=94, ∠HNiC=101, and ∠CCMe=126 for **10b**. Where L is H and X is OH, R(Ni–H)=1.506, R(Ni–P)=2.590, R(Ni–C)=1.972, R(C=C)=1.333, ∠HNiP=94, ∠HNiC=101, and ∠NiC-(OH)=119 for **10a**, R(Ni–H)=1.525, R(Ni–P)=2.606, R(Ni–C)=1.966, R(C=C)=1.324, ∠HNiP=93, ∠HNiC=100, and ∠CC(OH)=127 for **10b**. Where L is PH_3 and X is CH_3, R(Ni–P)=2.590, R(Ni–P^2)=2.566, R(Ni–C)=1.888, R(C=C)=1.327, ∠P^1NiP^2=100, ∠P^1NiC=100, and ∠NiCMe=105.2 for **10a**, R(Ni–P^1)=2.610, R(Ni–P^2)=2.572, R(Ni–C)=1.886, R(C=C)=1.329, ∠P^1NiP^2=100, ∠P^1NiC=97, and ∠CCMe=126 for **10b**. Where L is P^1H_3 and X is OH, R(Ni–P^1)=2.553, R(Ni–P^2)=2.552, R(Ni–C)=1.909, R(C=C)=1.322, ∠P^1NiP^2=93, ∠P^1NiC=124, and ∠NiC(OH)=113 for **10a**, R(Ni–P^1)=2.627, R(Ni–P^2)=2.568, R(Ni–C)=1.896, R(C=C)=1.331, ∠P^1NiP^2=99, ∠P^1NiC=96, and ∠CC(OH)=128.

32) When X is OH, **13a** is 10 kcal mol^{-1} more stable than **13b** for L=larger PH_3 but 2.5 kcal mol^{-1} more stable than **13b** for L=smaller H. This result can not be interpreted in terms of the steric repulsion from PH_3. Thus, relative stabilities of **13a** and **13b** would be influenced by the other factors, such as σ-electron releasing (or withdrawing) effects, electrostatic effects, etc. The substituent effects on σ-alkyl and vinyl complexes are interesting issues to be theoretically examined. We must carry out derailed investigation, which is in progress now.

33) a) Remember that even a chelate phosphine can become a monodentate ligand in the reaction.[33b] However, the rigid bpy ligand would be difficult to eliminate from Ni. b) Y. Ben-David, M. Portnoy, M. Gozin, and D. Milstein, *Organometallics*, **11**, 1995 (1995).